Journal of Applied Sciences

ISSN 1812-5654

science alert

ANSInet
an open access publisher
http://ansinet.com

Journal of Applied Sciences 7 (5): 663-670, 2007
ISSN 1812-5654

Aerodynamic Analyses of Different Wind Turbine Blade Profiles

Ferhat Kurtulmus, Ali Vardar and Nazmi Izli
Department of Agricultural Machinery, Faculty of Agriculture, Uludag University,
16059 Bursa, Turkey

Abstract: For thousands of years mankind is utilizing wind energy. Increasing world population and increasingly reducing oil reserves and resulting requirement for clean, reliable, renewable energy systems intensifies the requirement for wind energy in long term. Nowadays, wind turbines are used for transforming that energy into electrical and mechanical energy. In order to gain from a wind turbine economically in maximum amounts performance data based on blade cross-section characteristics must be found. In the present study angle of attacks for 4 various blade profiles, Re numbers and correlations between lift and drag rates are investigated. Snack 2.0, computer software has been used for the calculation of lift, drag, moment and minimum pressure coefficients. For all evaluated blade profiles and all Re rates in the provided highest sliding rates most convenient angle of attack was determined in the range of 3° and 9°. According to lift-drag correlation in constant drag value as long as Re rate is higher also lift is intensified. Highest drag rates found corresponding to Re 20000.

Key words: Wind turbine, rotor, blade profile, attack angle

INTRODUCTION

Mankind gains from wind energy for thousand years. Much earlier than the invention of internal combustion engines wind-driven ships were used. Actually, wind energy became significant in the energy crises experienced between 1973-1974 (Vardar, 2002; EIE, 2000). Increasing world population and increasingly deregulating oil reserves in long term necessity of reliable, clean, renewable energy systems intensified the requirement for wind energy.

Wind energy is termed as the kinetic energy of circulating air (Klug, 2001). Contemporarily, wind energy is used for transforming that energy into electricity and mechanical energy sources. Wind turbines are classified into two sub-groups as vertical and horizontal axis turbines. In the vertical axis wind turbine type Darrieus type and Cyclogiro type and Savonius type wind turbines are used most commonly. Horizontal axis wind turbines are classified into three classes as classic wind turbines, slow wind turbines and rapid wind turbines. Considering economic terms in energy production turbine type possessing significant impact is the horizontal axis wind turbine type. Rapid wind turbines are manufactured as 1, 2, 3 or 4 blades (EIE, 1992).

Wind turbines on the propeller blades possess various blade profiles such as NACA, LS and LM profiles standards. In horizontal axis wind turbines NACA profiles standards of National Advisory Committee for Aeronautics is applied. There are a lot of forces effecting those profiles. In Fig. 1, forces influencing blade profile in fixed form are depicted.

Establishment of a wind turbine plant requires high expenses. Many initially designed parameters may be changed following the constructions. Thus, many variables must be taken into account and optimum design parameters must be confirmed and commence to the establishment of the plants. In order to gain from a wind turbine in cost saving way in addition to optimum operation parameters performance data, related to blade cross-section characteristics must be depicted.

In Fig. 1, r diameter blade section and based on the position with the wind provided powers and angles are depicted. Relativistic wind vector in r diameter (W) is the (ur) component of the axis component (uP) and rotating component (ur). Angle of attack is depicted as α and θ represents the blade connection angle. Angle composed by blade rotation vertical angle and relativistic vector corresponds to Φ. As can be seen lift (C_L) and drag (C_D) power components are parallel to power components according to relativistic wind vector in vertical and parallel positions respectively (Lee and Flay, 1999).

One of the significant factor for blade profile is the chord length. Chord length is the length between leading edge and trailing edge (Fig. 2). Chord length may have various values at the square and end points on the blade (Desktop Aeronautics, 2006).

Corresponding Author: Ali Vardar, Department of Agricultural Machinery, Faculty of Agriculture, Uludag University, 16059 Bursa, Turkey Tel: +90 224 442 98 70 (381) Fax: +90 224 442 91 49

Tip speed ratio is correlated with circumference speed in r distance of the rotor from the center of the rotor, wind speed, angle speed and propeller diameter and as a non-dimensional magnitude expressed in the formula below (Vardar and Eker, 2004).

$$\lambda = \frac{\omega.R}{v_1} \quad (1)$$

NACA blade profiles are defined based on some of the parameters (Table 1). Those are as seen in Fig. 1 presented in the example given for NACA 4412 are maximum slope percentage of the chord, maximum position of the slope and maximum thickness of the chord in percentage.

Table 1: Meaning of profile codes for NACA 4412 blade profiles

4	4	1	2
max camber in % chord	position of max camber in 1/10 of chord	max thickness in % of chord	

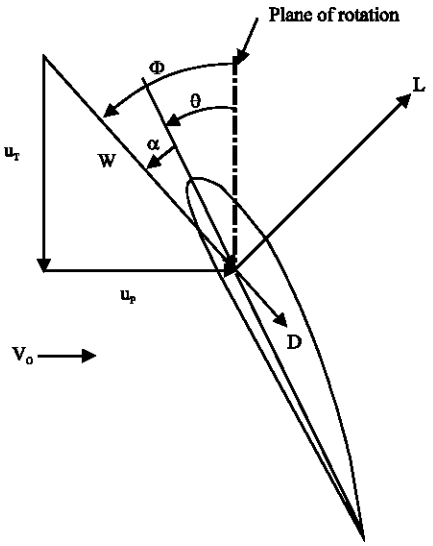

Fig. 1: Blade element force velocity diagram

Purpose of that study is to present the aerodynamic properties of the blade cross-sections as a one of the most crucial parameters of a wind turbine plant. Some of the NACA profiles are selected and most optimum Re value angle of attack, profile chord length, sliding rate, lift and drag coefficients, moment and minimum pressure coefficients have been taken into concern. In order to find out lift, drag, moment and minimum pressure coefficients Snack 2.0 computer software is used.

MATERIALS AND METHODS

Nowadays, wind turbines blade numbers change in the range of 2 and 24 rotor diameters vary in the range of 2 and 100 m (Table 2). When those ranges are considered further to Re rate chord lengths varies in the range of 0.1 and 5 m. In the Eq. (2) as can be seen, Re number is connected to Chord length of the rotor wind profile and wind speed (Piggott, 1998).

$$Re = 68500 \cdot C \cdot v \quad (2)$$

Chord value is correlated with rotor diameter, blade numbers on the rotor and rotor tip speed ratio (Piggott, 1998).

$$C = \frac{4.D}{\lambda^2.B} \quad (3)$$

Rotor tip speed ratio varies based on the blade numbers on the rotor (Piggott, 1998).

$$\lambda = \sqrt{\frac{80}{B}} \quad (4)$$

In the present study some of the blade profiles are selected submitted by NACA (Dresse, 2000). Those selected profiles are NACA 0012, NACA4412, NACA 4415 and NACA23012 and depicted in Fig. 3.

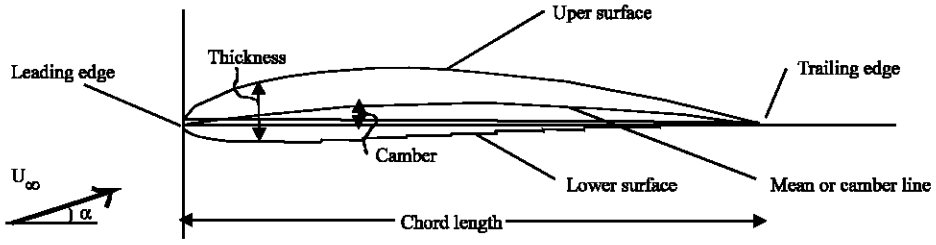

Fig. 2: Geometrical parameters of a wind turbine's blade profiles

Table 2: Re numbers taken in that study as a base rate

	Re number
1	20.000
2	60.000
3	100.000
4	150.000
5	500.000
6	1.000.000
7	2.000.000
8	3.000.000
9	4.000.000
10	5.000.000
11	6.000.000
12	7.000.000
13	8.000.000
14	9.000.000

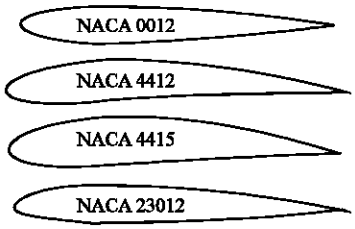

Fig. 3: Selected profiles

In the present study by Snack 2.0 computer program lift and drag angles for the selected wind turbine profiles are calculated in the range of 0 and 20 degree angle of attack. Those calculated values plotting into the equation below sliding angle (ϵ) is found for the angle of attack for each profile (Ozdamar and Kavas, 1999).

$$\varepsilon = \frac{C_L}{C_D} \quad (5)$$

Considering the Re figures provided by means of the equations depicted above for each blade profiles minimum and maximum ranges for Re figure have been calculated. In those ranges for each blade profiles at 14 various Re figures correlations between angle of attack and sliding figures have been calculated. Also by those equations for each blade profiles most available angle of attack values have been determined. For the most optimum angle of attack calculated correlations between Re figures and correlation between each profile's lift rate and angle of attack are presented in a chart form.

Later on for the most available angle of attack again Snack 2.0 Computer program is gained for calculating the moment and minimum pressure coefficients of the profiles have been calculated (Table 3).

At the end of the studies performed for each of the Re figures profile angle of attack sliding figure charts and charts for Re figure and angle of attack have been calculated.

Table 3: Lifting and drifting coefficients of blade profiles and differentiation of moment and minimum pressure coefficient rates for the best angle of attack they provide depending on Re value

Profile name	Attack angle (α)	Moment	Minimum Pressure Coefficient
NACA 0012	3	-0.0049	-1.038
	4	-0.0065	-1.41
	5	-0.0081	-1.868
	6	-0.0097	-2.365
	7	-0.0112	-3.048
	8	-0.0128	-3.799
	9	-0.0143	-4.611
NACA 4412	3	-0.1166	-1.122
	4	-0.1184	-1.334
	5	-0.1203	-1.686
	6	-0.1222	-2.172
	7	-0.124	-2.705
	8	-0.1259	-3.373
	9	-0.1278	-4.164
NACA 4415	3	-0.1189	-1.253
	4	-0.1213	-1.422
	5	-0.1236	-1.656
	6	-0.126	-1.981
	7	-0.1284	-2.38
	8	-0.1308	-2.856
	9	-0.1332	-3.406
NACA 23012	3	-0.0154	-1.175
	4	-0.0171	-1.387
	5	-0.0189	-1.642
	6	-0.0206	-1.952
	7	-0.0224	-2.356
	8	-0.0243	-2.898
	9	-0.0261	-3.503

RESULTS AND DISCUSSION

In the present study primarily Re figures for a wind turbine rotor have been calculated. In our present time wind turbines may produce energy only between 3 m s^{-1} and 25 m s^{-1} wind speed range. Re figures have to be considered are determined corresponding to 20,550 and 8,562,500 values and in the present study that range have been taken into concern. Re values have to be taken into concern are depicted in Fig. 2.

Blade profile's lift and drag coefficients and based on Re their moment and minimum and maximum pressure coefficient ratios they provide for best angle of attack are depicted in Fig. 3.

For Re 20000 and 9000000 correlations between sliding ratio and angle of attack are depicted in Fig. 4-17.

In Fig. 4 for Re 20000, most available angle of attack figures at the highest sliding figures provided by the use of NACA 0012, NACA 4412 and NACA 4415 are depicted. Those figures for NACA 4412 has been found as 5°, for NACA 4415 6°, for NACA 23012 8° and for NACA 0012 9°.

In Fig. 5 for Re 60000, most available angle of attack figures at the highest sliding ratios by using NACA 0012, NACA 4412, NACA 4415 and NACA 23012 have been found as 8°, 4°, 5° and 7°.

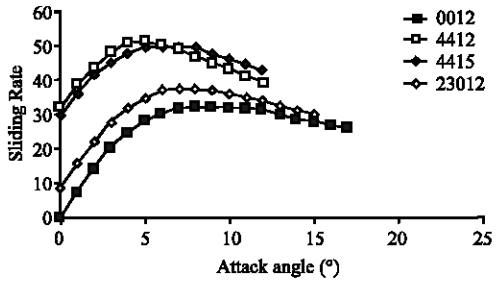

Fig. 4: Correlation between sliding rate and angle of attack for Re 20000

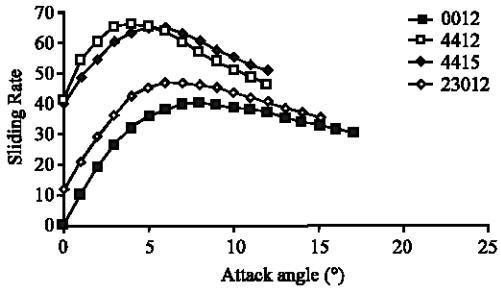

Fig. 5: Correlation between sliding rate and angle of attack for Re 60000

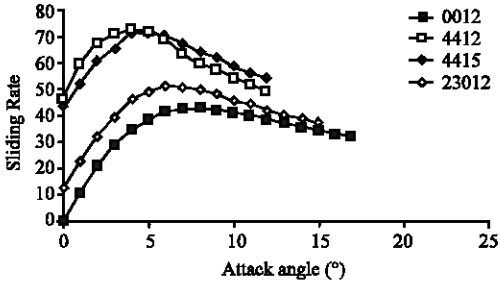

Fig. 6: Correlation between sliding rate and angle of attack for Re 100000

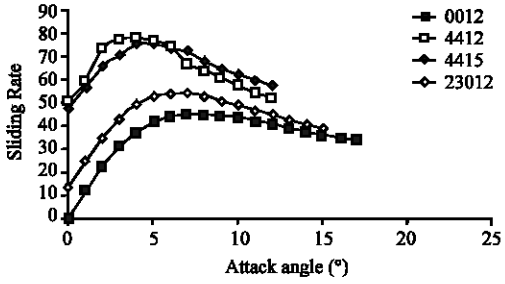

Fig. 7: Correlation between sliding rate and angle of attack for Re 150000

In Fig. 6, for Re 100000 most convenient angle of attack was corresponding to 4° at the highest sliding value for NACA 4412 and NACA 4415 profiles and for NACA 23012 profile it was corresponding to 6° and for NACA 0012 found as 8°.

In Fig. 7 for Re 150000 at the highest sliding figures most convenient angle of attack ratios were respectively 7°, 4°, 5° and 6° at the highest sliding rates provided by using NACA 0012, NACA 4412, NACA 4415 and NACA 23012.

In Fig. 8 for Re 500000 most convenient angle of attack are found as 7°, 3°, 4° and 6° respectively at the highest sliding figures by using NACA 0012, NACA4412, NACA 4415 and NACA 23012 profiles.

In Fig. 9 and 10, when Re 1000000 and Re 2000000 are taken into account most convenient angle of attack values are found respectively as 6°, 4°, 4° at the highest sliding values provided by using NACA 0012, NACA 4412 and NACA 4415 profiles. For NACA 23012 profile at the Re 1000000 it was calculated as 6° and for Re 2000000 it was found as 5°.

In Fig. 11-16 most convenient angle of attack were 7° and 3° at the highest sliding rates provided by using NACA 0012 and NACA 4412 for 3000000, 4000000, 5000000, 6000000, 7000000 and 9000000 for NACA 4415 that ratio lies on a line in the range of 5° and 4°. For

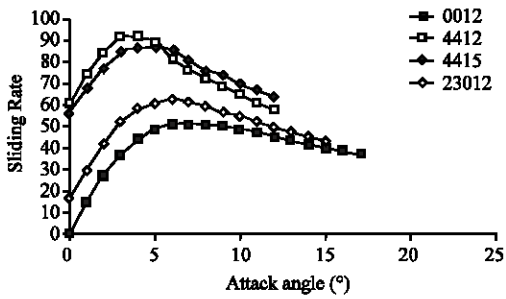

Fig. 8: Correlation between sliding rate and angle of attack for Re 500000

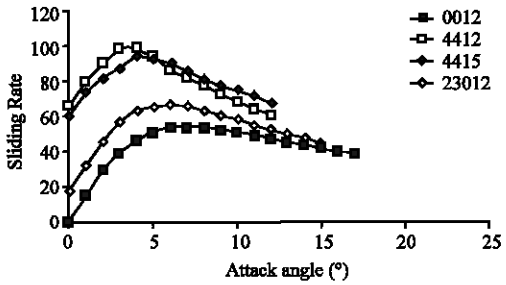

Fig. 9: Correlation between sliding rate and angle of attack for Re 1000000

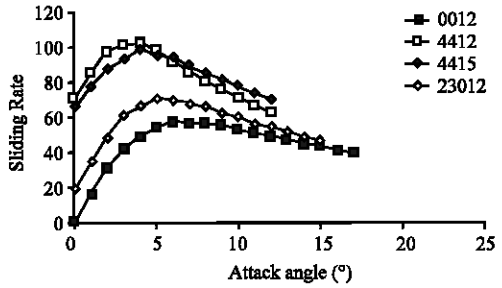

Fig. 10: Correlation between sliding rate and angle of attack for Re 2000000

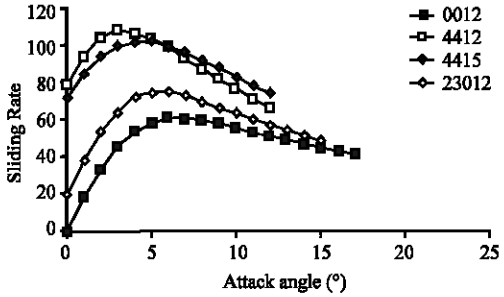

Fig. 14: Correlation between sliding rate and angle of attack for Re 6000000

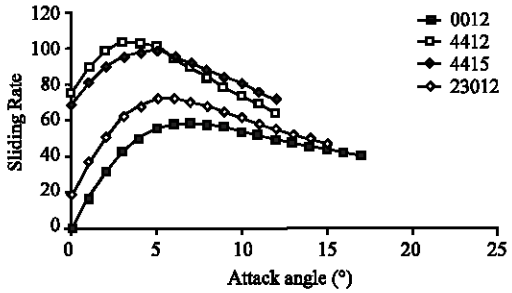

Fig. 11: Correlation between sliding rate and angle of attack for Re 3000000

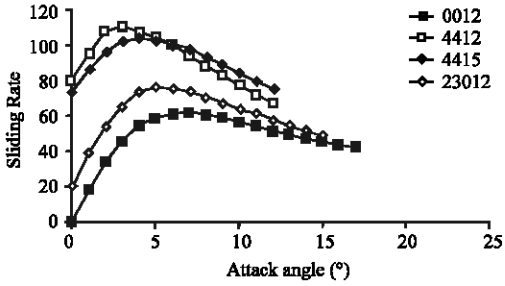

Fig. 15: Correlation between sliding rate and angle of attack for Re 7000000

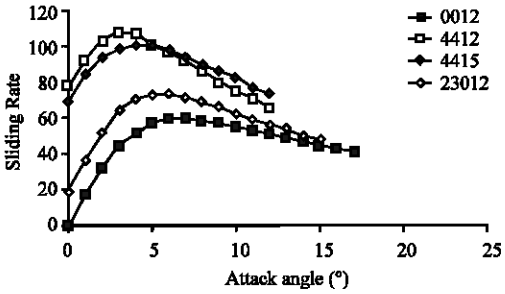

Fig. 12: Correlation between sliding rate and angle of attack for Re 4000000

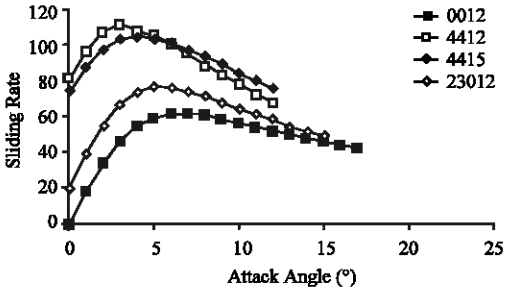

Fig. 16: Correlation between sliding rate and angle of attack for Re 8000000

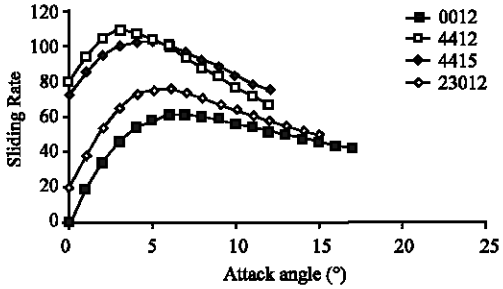

Fig. 13: Correlation between sliding rate and angle of attack for Re 5000000

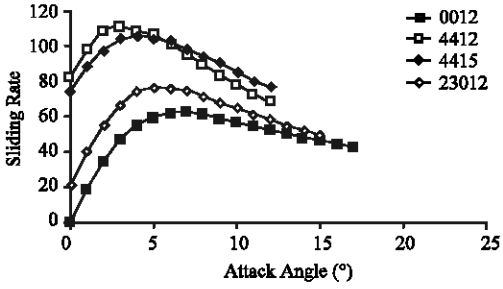

Fig. 17: Correlation between sliding rate and angle of attack for Re 9000000

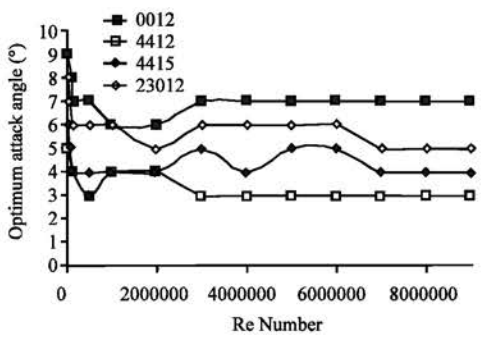

Fig. 18: Correlation between optimum angle of attack and Re numbers

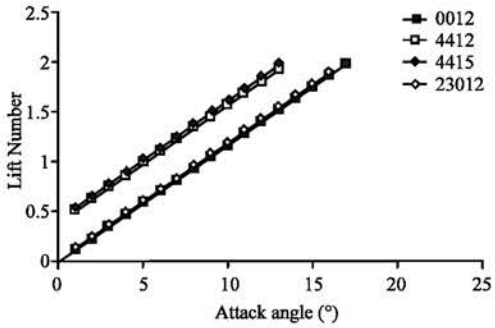

Fig. 19: Correlation between lifting rate of the profiles and angle of attack

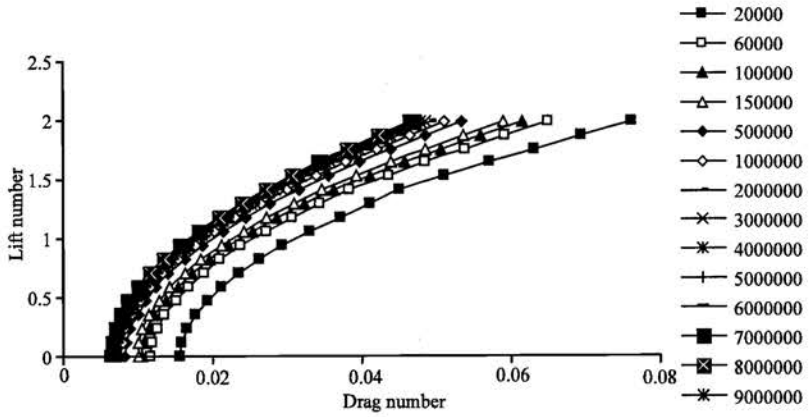

Fig. 20: Correlation between lifting and drifting rate for NACA 0012

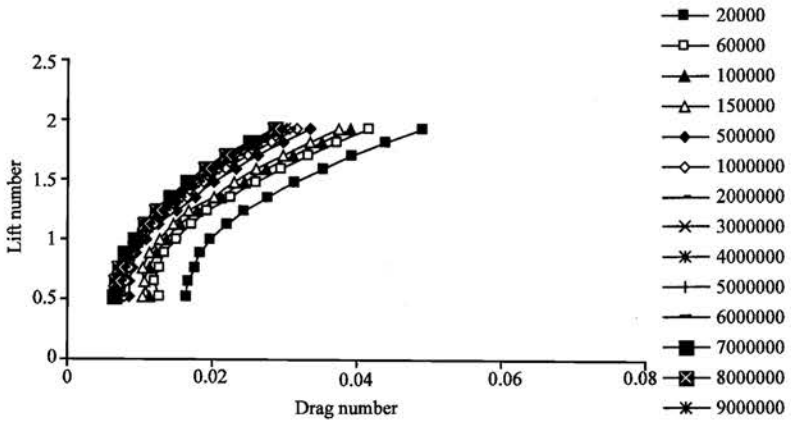

Fig. 21: Correlation between lifting and drifting rat for NACA 4412

NACA 23012 profile that value was seen as 6° at the beginning and when the Re figure is increasing it remained constant at 5°.

Correlation between Re and most convenient angle of attack is depicted in Fig. 18. On NACA 0012 profile, based on Re figures most convenient angle of attack for Re 20000 and 3000000 while remain in range of 6° and 9°, remain constant for Re 3000000 and Re 9000000 at 7°. In similar way for NACA 4412 profile further to Re figures most convenient angle of attack between Re 20000 and 3000000 varies in 5° and 3°, between Re 3000000 and 9000000 remains constant at 3°. Generally, for the entire

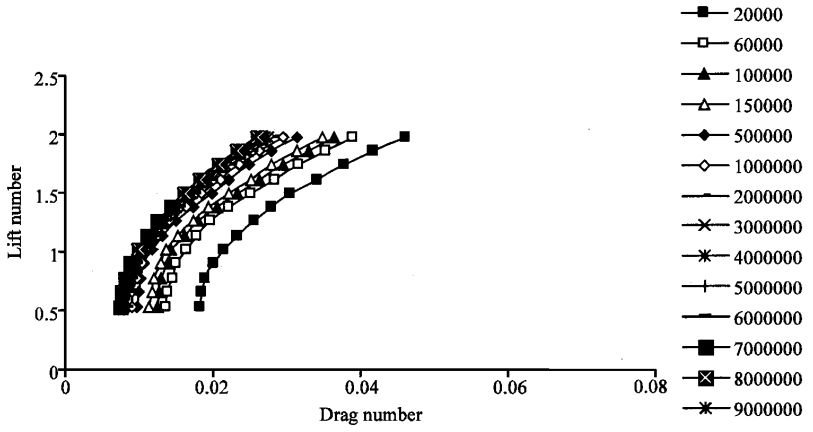

Fig. 22: Correlation between lifting and drifting rate for NACA 4415

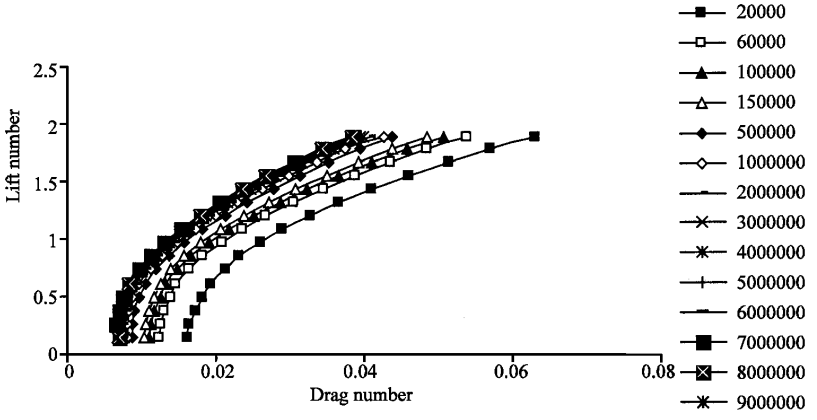

Fig. 23: Correlation between lifting and drifting rate for NACA 23012

profiles according to Re figures most convenient angle of attack is variable up to Re 3000000 and beyond Re 3000000 value they are found constant at an angle rate.

For NACA 0012, NACA 4412, NACA 4415 and NACA 5317 profiles correlation between lift rate and angle of attack is depicted in Fig. 19. For NACA 4412 and NACA 4415 from 1 to 20 lift rates based on angle of attack are very close to each other. In a similar way, lift rates for NACA 0012 and NACA 23012 are also found very closer to each other. For NACA 4412 and NACA 4415 lift rates corresponding to same angle of attack are much higher than NACA 0012 and NACA 23012.

At the Re figures of the profiles in the range of 20000 and 9000000 correlation between lift and drag rates are depicted in Fig. 20-23. As can be seen from the figures corresponding to rising up Re ratios lift rates remain constant but drag rates fall down. As can be seen from the charts corresponding to rising Re values lift rate remains stable and drag values fall down. Based on the lift-drag correlations at the constant drag values, increase in Re value leads to increase in lift. Highest drag values are provided at Re 20000 level.

RESULTS

In the present study for 4 different blade profiles angle of attack, Re rates, lifting and drag values are investigated based on their correlations. For all blade profiles and all Re values at the highest sliding rates most convenient angle of attack values are found in the range of 3° and 9°. Most convenient blade angle up to Re 3000000 rate found varying between 3° and 9°, after Re 3000000 point remains constant in the range of 3° and 7°. Moment and minimum pressure coefficients minimum moment and minimum pressure coefficient are seen on NACA 0012 profile at the 3° angle of attack. Highest moment has been found on the NACA 4415 profile in the first 9° angle of attack and the highest minimum pressure coefficient found on the NACA 23012 profile in the first 9° angle of attack. Against the

increasing Re values lift values remain constant and drag coefficients remains falling. Highest drag values are found on Re 20000 value. Based on the lift-drag correlation in constant drag values as Re rises up also lift rises up in accordance.

NOMENCLATURE

W	:	The relative wind vector at radius r
uP	:	Axial component of W
uT	:	Rotational component of W
θ	:	The pitch of the blade
C_L	:	Lifting Coefficient
C_D	:	Drag Coefficient
ω	:	Angular velocity (degree)
R	:	Radius (m)
ε	:	Sliding Number
C	:	Chord length (m)
D	:	Rotor Diameter (m)
B	:	Blade Number
λ	:	Tip speed ratio
Re	:	Reynold Number
V	:	Wind Speed (ms^{-1})
V_1	:	Wind speed front the rotor (ms^{-1})
ϕ	:	The angle of the relative wind to the plane of rotation
NACA	:	National Advisory Committed For Aeronautics

REFERENCES

Desktop Aeronautics, 2006 Desktop Aeronautics, 2006. Applied Aerodynamics: A Digital Textbook, www.desktopaero.com/appliedaero/airfoils1/airfoilgeometry.html

Dresse, J., 2000. Aero Basics and DesignFOIL, User Guide, Capitola, California.

EIE., 1992. Wind Energy, Electrical Power Resources Survey and Development Administration, Ankara.

EIE., 2000. Mechanical conversion systems of wind energy in water pumping operation, Electrical Power Resources Survey and Development Administration, Ankara.

Klug, H., 2001. Basic Course in Wind Energy. German Wind Energy Institute GmbH (DEWI), Istanbul.

Lee, A.T. and R.G.J. Flay, 1999. Compliant blades for wind turbines. IPENZ Transactions, 1999, Vol. 26, No. 1/EMCh.

Özdamar, A. and M.G. Kavas, 1999. A Reseach of Wind Turbine Rotor Design, Sun Day Symposium, 25-27 June 1999, Kayseri, Turkey.

Piggott, H., 1998. See also: http://homepages. enterprise. net/hugh0piggott/wpNotes/index.htm

Vardar, A., 2002. A research on determination of the fittest blade type, blade angle and blade position for establishing a wind turbine with agricultural aim in trakya region. University of Trakya, Institute of Science, Branch of Agriculture Machines Ph.D. Thesis, Tekirdag.

Vardar, A. and B. Eker, 2004. The Wind Measuring Methods For Wind Turbine Rotor Blades, Wind and Structures, An International J. 7: 305-316.